CHINESE JOURNAL OF PHYSICS VOL. 37, NO. 3 JUNE 1999

# A Modified BFKL Equation With Q Dependence

Jyh-Liong Lim [1] and Hsiang-nan Li [2]
[1] Department of Electrophysics, Nationai Chiao-Tung University, Hsinchu, Taiwan 300, R.O.C.
[2] Department of Physics, National Cheng-Kung University, Tainan, Taiwan 701, R.O. C.

(Received September 17, 1998)

We propose a modified Balitsky-Fadin-Kuraev-Lipatov (BFKL) equation for the summation of large $\ln(1/x)$, $x$ being the Bjorken variable, which contains an extra dependence on the momentum transfer Q compared to the conventional BFKL equation. This Q dependence comes from the phase space constraint for soft real gluon emissions in the derivation of the BFKL kernel. The modified equation gives a slower rise of the gluon distribution function with $1/x$ for smaller Q, such that the predictions for the structure functions $F_{2,L}(x,Q^2)$ involved in deep inelastic scattering match the HERA data. These results are similar to those obtained from the Ciafaloni-Catani-Fiorani-Marchesini equation, which embodies both the ln Q and ln( $1/x$) summations. The reason that the conventional BFKL equation can not be applied to the low Q (soft pomeron dominant) region is given.

PACS. 12.38.Bx – Perturbative calculations.
PACS. 12.38.Cy – Summation of perturbation theory.

## I. Introduction

The deep inelastic scattering (DIS) experiments performed at HERA [1] have stimulated many intensive discussions on the behavior of the structure function $F_2(x,Q^2)$ at small Bjorken variable $x$ for various values of the momentum transfer Q. One of the important subjects is to explain the data of $F_2$ using the known evolution equations. In the low $x$ region with $\ln(1/x) \gg \ln Q$, the appropriate tool is the Balitsky-Fadin-Kuraev-Lipatov (BFKL) equation [2] which sums large $\ln(1/x)$ in the gluon distribution function to all orders. Since the BFKL equation does not depend on the momentum transfer explicitly, its predictions for the gluon distribution function and for $F_2$ exhibit a weak Q dependence. However, the HERA data show that the rise of $F_2$ at small $x$ varies with Q in a more sensitive way: The ascent is rapid for large Q, which is attributed to hard (or BFKL) pomeron contributions. The slow ascent at low Q, which can not be explained by the BFKL equation, is interpreted as the consequence of soft pomeron exchanges.

To understand the Q-dependent rise of the gluon distribution function and of the structure function, the Dokshitzer-Gribov-Lipatov-Altarelli-Parisi (DGLAP) equation [3] for the $\ln Q$ summation should be included somehow. One may resort to the DGLAP equation directly, because the relevant splitting function $P_{gg} \propto 1/x$ also gives an increase

at small $x$. However, the DGLAP **rise is** milder, and a steep nonperturbative input of the gluon distribution function at low Q must be adopted. An alternative is the $p_T$-factorization theorem [4], which has been shown to be equivalent to the collinear (mass) factorization, the framework on which the DGLAP equation is based. By including the next-to-leading $\ln(1/x)$ from singlet quark contributions, the rise becomes faster, and a flat input is proposed [5]. The double scaling tendency exhibited by the predictions from the DGLAP equation with the next-to-leading logarithms taken into account and by the data of $F_2$ has been explored [6]. The conclusion also favors a flat nonperturbative input. The above investigations imply that the structure function at low Q is dominated by soft pomeron contributions, and the large-Q behavior is the result of the DGLAP evolution.

Another possibility is the Ciafaloni-Catani-Fiorani-Marchesini (CCFM) equation [7], which embodies the BFKL equation for small $x$ (and intermediate Q) and the DGLAP equation for large Q (and intermediate $x$). To derive the CCFM equation, the angular ordering of rung gluons in ladder diagrams is assumed, which can be regarded as a combination of the rapidity ordering for the BFKL equation and the transverse momentum ordering for the DGLAP equation. The CCFM equation has been studied in details in [8]. It is found that the resultant gluon distribution function shows the desired Q dependence, and the predictions for $F_2$ are in agreement with the HERA data. This equation, though considering only the gluon contributions, predicts a steeper rise than the DGLAP equation does, since the running coupling constant involved in the splitting function is evaluated at the gluon transverse momentum, instead of at Q.

The above analyses, though consistent with the data, did not address the issue why the BFKL equation can not be applied to DIS in the low Q region, where it is supposed to be more appropriate because of $\ln(1/x) \gg \ln Q$. **In** this paper we shall derive the BFKL equation in an alternative way from the viewpoint of the Collins-Soper-Sterman resummation technique [9]. By truncating the loop momenta of real gluons at Q in the evaluation of the evolution kernel, a modified equation is obtained. Since real gluon emissions are responsible for the BFKL rise, the rise is rendered slower at smaller Q, where the phase space for real gluon emissions is more restricted. We argue that this is a plausible reason the conventional BFKL equation, overestimating real gluon contributions, fails in the low Q region. The modified equation is simpler than the CCFM equation, and explains the HERA data of the structure functions $F_{2,L}$ well.

In Sect. II we derive the Q-dependent BFKL equation using the resummation technique, and show that it approaches the conventional one as the cutoff of the loop momenta is removed. In Sect. III the evolution of the gluon distribution function in $x$ predicted by the modified BFKL equation is compared with those by the DGLAP equation, the conventional BFKL equation, and the CCFM equation. The modified BFKL equation is solved numerically, and the results of the gluon distribution function and of the structure functions $F_{2,L}$ are presented in Sect. IV. Section V is the conclusioin, and the Appendix contains the details of the involved calculations.

## II. Formalism

In [10,11] **we** have proposed a unified derivation of the known evolution equations that sums various large logarithms based on the resummation technique [9], such as the

DGLAP, BFKL, CCFM, and Gribov-Levin-Ryskin (GLR) equation [12]. The GLR equation includes the annihilation effect of two gluons into one gluon in the region with Q and $1/x$ being simultaneously large. Briefly speaking, the resummation technique relates the derivative of a parton distribution function to a new function involving a special vertex [9, 13]. The new function is then expressed as a factorization formula involving the subdiagram containing the special vertex and the original distribution function. Evaluating the subdiagram according to some specific ordering of radiative gluons, the derivative of the distribution function turns into the corresponding evolution equation. The complexity of the conventional derivation of the evolution equations is thus greatly reduced.

In this section we apply the above formalism to DIS of a proton with light-like momentum $P^\mu = P^+\delta^{\mu+}$ in the small $x$ limit, where $x = -q^2/(2P \cdot q) = Q^2/(2P \cdot q)$ is the Bjorken variable, $q$ being the momentum of the photon. The unintegrated gluon distribution function $F(x, k_T)$, describing the probability of a gluon carrying a longitudinal momentum fraction $x$ and transverse momentum $p_T$, is defined by

$$F(x, p_T) = \frac{1}{P^+}\int \frac{dy^-}{2\pi}\int \frac{d^2y_T}{4\pi} e^{-i(xP^+y^- - p_T\cdot y_T)} \times \langle P|F_\mu^+(y^-, y_T)F^{\mu+}(0)|P\rangle , \tag{1}$$

in the axial gauge $n \cdot A = A^+ = 0$, $n = \delta^{\mu-}$ being a vector on the light cone. The ket $|P\rangle$ denotes the incoming proton, and $F_\mu^+$ is the field tensor. Averages over the spin and color are understood. To implement the resummation technique, we allow n to vary away from the light cone ($n^2 \neq 0$) first. It will be shown that the BFKL kernel turns out to be n-independent. After deriving the evolution equation, n is brought back to the light cone, and the definition of the gluon distribution function coincides with the standard one [14]. That is, the arbitrary vector n appears only at the intermediate stage of the derivation and as an auxiliary tool of the resummation technique.

Though $F$ at $x \to 0$ does not depend on $P^+$ explicitly as shown later, it varies with $P^+$ through the momentum fraction implicitly, which is proportional to $(P^+)^{-1}$. Hence, the derivative $P^+dF/dP^+$ can be written as

$$P^+\frac{d}{dP^+}F(x, P_T) \equiv -x\frac{d}{dx}F(x, P_T) \tag{2}$$

Because of the scale invariance of $F$ in n, as indicated by the gluon propagator, $(-i/l^2)N^{\mu\nu}(l)$, with

$$N^{\mu\nu} = g^{\mu\nu} - \frac{n^\mu l^\nu + n^\nu l^\mu}{n\cdot l} + n^2\frac{l^\mu l^\nu}{(n\cdot l)^2} , \tag{3}$$

$F$ must depend on $P$ via the ratio $(P \cdot n)^2/n^2$. We then have the chain rule relating $P^+d/dP^+$ to $d/dn$ [9.13],

$$P^+\frac{d}{dP^+}F = -\frac{n^2}{v\cdot n}v_\beta\frac{d}{dn_\beta}F , \tag{4}$$

$v_\beta = \delta_{\beta+}$ being a vector along $P$. The operator $d/dn_\beta$ applying to the gluon propagator gives

$$\frac{d}{dn_\beta}N^{\nu\nu'} = -\frac{1}{n\cdot l}(l^\nu N^{\beta\nu'} + l^{\nu'}N^{\nu\beta}) . \tag{5}$$

The loop momentum 1" ($l^{\nu'}$) contracts with the vertex the differentiated gluon attaches, which is then replaced by a special vertex

$$\hat{v}_\beta = \frac{n^2 v_\beta}{v\cdot n n\cdot l} . \tag{6}$$

This special vertex can be read off from the combination of Eqs. (4) and (5).

The contraction of 1" hints the application of the Ward identities [10,11],

$$\frac{i(\not k+\not l)}{(k+l)^2}(-i\not l)\frac{i\not k}{k^2} = \frac{i\not k}{k^2} - \frac{i(\not k+\not l)}{(k+l)^2} , \tag{7}$$

for the quark-gluon vertex, and

$$l^\nu \frac{-iN^{\alpha\mu}(k+l)}{(k+l)^2}\Gamma_{\mu\nu\lambda}\frac{-iN^{\lambda\gamma}(k)}{k^2} = -i\left[\frac{-iN^{\alpha\gamma}(k)}{k^2} - \frac{-iN^{\alpha\gamma}(k+l)}{(k+l)^2}\right] , \tag{8}$$

for the triple-gluon vertex $\Gamma_{\mu\nu\lambda}$. The Ward identity for the four-gluon vertex,

$$\begin{aligned}\Gamma^{abcd}_{\lambda\mu\nu\sigma} \propto\ & f^{abe}f^{cde}(g_{\lambda\nu}g_{\mu\sigma} - g_{\lambda\sigma}g_{\mu\nu}) + f^{ace}f^{bde}(g_{\lambda\mu}g_{\nu\sigma} - g_{\lambda\sigma}g_{\mu\nu}) \\ & + f^{ade}f^{cbe}(g_{\lambda\nu}g_{\mu\sigma} - g_{\lambda\mu}g_{\sigma\nu}) ,\end{aligned} \tag{9}$$

is simpler. The sum of the four contractions from $l_1^\lambda, l_2^\mu, l_3^\nu$, and $l_4^\sigma$ to the four-gluon vertex vanishes: The contractions from $l_1^\lambda$ and $l_2^\mu$ to the first term of $\Gamma^{abcd}_{\lambda\mu\nu\sigma}$ cancel each other. because the first term is antisymmetric with respect to the interchange of the indices $\lambda$ and $\mu$. Similar cancellation occurs between the contractions from $l_3^\nu$ and $l_4^\sigma$. The contractions from $l_1^\lambda$ and $l_3^\nu$ and from $l_2^\mu$ and $l_4^\sigma$ to the second term cancel separately. The contractions from $l_1^\lambda$ and $l_4^\sigma$ and from $l_2^\mu$ and $l_3^\nu$ to the third term also cancel separately.

Summing the diagrams with different differentiated gluons, those embedding the special vertices cancel by pairs, leaving the one where the special vertex moves to the outer end of the parton line [9]. We obtain the formula,

$$-x\frac{d}{dx}F(x,p_T) = 2\bar{F}(x,p_T) , \tag{10}$$

described by Fig. l(a), where the new function $\bar{F}$ contains one special vertex represented by a square. The coefficient 2 comes from the equality of the new functions with the special vertex on either of the two parton lines. Note that Eq. (10) is an exact consequence of the Ward identities without approximation [9]. An approximation will be introduced, when $\bar{F}$ is related to $F$ by factorizing out the subdiagram containing the special vertex, such that Eq. (10) reduces to a differential equation of $F$.

It is known that factorization holds in the leading regions. The leading regions of the loop momentum $l$ flowing through the special vertex are soft and hard, since the factor

$1/n\cdot l$ with $n^2\neq 0$ in Eq. (6) suppresses collinear divergences [9]. For soft and hard $l$, the subdiagram containing the special vertex is factorized according to Figs. l(b) and l(c), respectively. Fig. l(b) collects the soft divergences of the subdiagram by eikonalizing the gluon propagator, which will be explained below. We extract the color factor from the relation $f_{abc}f_{bdc}=-N_c\delta_{ad}$, the indices a, $b,\ldots$ being indicated in Fig. l(b), and $N_c=3$ the number of colors. The corresponding factorization formula is written as

$$\tilde{F}_s(x,p_T)=iN_cg^2\int\frac{d^4l}{(2\pi)^4}\Gamma_{\mu\nu\lambda}\hat{v}_\beta[-iN^{\nu\beta}(l)]\frac{-iN^{\lambda\gamma}(xP)}{-2xP\cdot l}\times\left[2\pi i\delta(l^2)F(x+l^+/P^+,|p_T+l_T|)+\frac{\theta(p_T^2-l_T^2)}{l^2}F(x,p_T)\right], \tag{11}$$

where $iN_c$ comes from the product of the overall coefficient -i in Eq. (8) and the color, factor $-N_c$ extracted above, g is the coupling constant, and the triple-gluon vertex for vanishing $l$ is given by

$$\Gamma_{\mu\nu\lambda}=-g_{\mu\nu}xP_\lambda-g_{\nu\lambda}xP_\mu+2g_{\lambda\mu}xP_\nu\ . \tag{12}$$

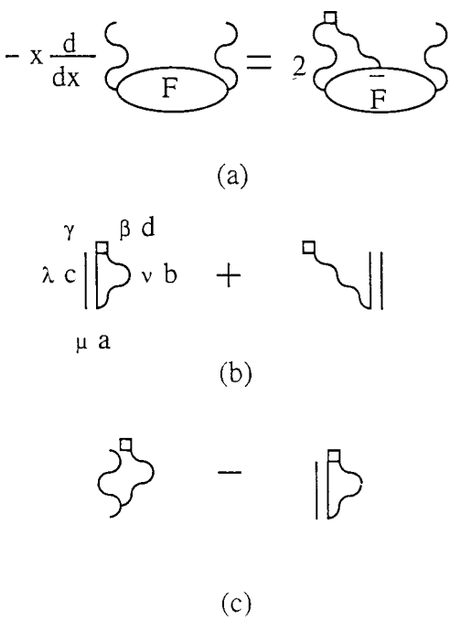


FIG. 1. (a) The derivative $-xdF/dx$ in axial gauge. (b) The soft structure and (c) the ultraviolet structure of the $O(\alpha_s)$ subdiagram containing the special vertex.

The denominator $-2xP\cdot l$ comes from the eikonal approximation $(xP-l)^2 \approx -2xP\cdot l$. The first term in the brackets corresponds to the real gluon emission, where $F(x+l^+/P^+, |p_T + l_T|)$ implies that the parton coming out of the proton carries the momentum components $xP^+ + l^+$ and $p_T + l_T$ in order to radiate a real gluon of momentum $l$. The second term corresponds to the virtual gluon emission, where the $\theta$ function sets the upper bound of $l_T$ to $p_T$ to ensure a soft momentum flow.

It can be easily shown that the contraction of $P$ with a vertex in the quark box diagram the partons attach, or with a vertex in the gluon distribution function, gives a contribution down by a power $1/s$, $s=(P+q)^2$, compared to the contribution from the contraction with $\hat{v}_\beta$. Following this observation, Eq. (11) is reexpressed as

$$\bar{F}_s(x,p_T) = iN_c g^2 \int \frac{d^4l}{(2\pi)^4} N^{\nu\beta}(l) \frac{\hat{v}_\beta v_\nu}{v\cdot l} \left[ 2\pi i\delta(l^2) F(x+l^+/P^+, |p_T+l_T|) + \frac{\theta(p_T^2-l_T^2)}{l^2} F(x,p_T) \right] . \tag{13}$$

The eikonal vertex $v_\nu$ comes from the term $xP_\nu$ (divided by $xP^+$) in Eq. (12), and the eikonal propagator $1/v\cdot l$ from $1/(xP\cdot l)$, which is represented by a double line in Fig. 1(b). The remaining metric tensor $g^{\mu\gamma}$ is multiplied by the tensor carried by the gluon just coming out of the proton, say, $g^\delta_\mu$, giving $g^{\delta\gamma}$. This new tensor is then associated with the gluon coming out of the proton, and absorbed into $F$.

We then approximate $F(x+l^+/P^+, |p_T+l_T|)$ by its dominant value $F(x, |p_T+l_T|)$. The integration over $l^-$ and $l^+$ to infinity gives

$$\begin{aligned} \bar{F}_s(x,k_T) &= \frac{\bar{\alpha}_s}{2} \int \frac{d^2l_T}{\pi} \frac{-n^2}{2n^-[n^+l_T^2 + 2n^-l^+2]} \Big|_{l^+=0}^{l^+=\infty} \\ &\quad \times [F(x,|k_T+l_T|) - \theta(k_T^2-l_T^2)F(x,k_T)] , \\ &= \frac{\bar{\alpha}_s}{2} \int \frac{d^2l_T}{\pi l_T^2} [F(x,|k_T+l_T|) - \theta(k_T^2-l_T^2)F(x,k_T)] , \end{aligned} \tag{14}$$

with $\bar{\alpha}_s = N_c\alpha_s/\pi$. The gauge vector $n=(n^+,n^-,0)$ has been assumed for convenience. The first line of the above formulas demonstrates explicitly how the $n$ dependence disappears in the evaluation of Fig. 1(b).

It can be shown that the contribution from the first diagram of Fig. 1(c) vanishes like [11]

$$-\frac{\bar{\alpha}_s}{2} \int \frac{d^2l_T}{\pi} \left[ \frac{1}{l_T^2} - \frac{1}{l_T^2 + (xP^+\nu)^2} - \frac{1}{2} \frac{xP^+\nu}{[l_T^2+(xP^+\nu)^2]^{3/2}} \ln \frac{\sqrt{l_T^2+(xP^+\nu)^2} - xP^+\nu}{\sqrt{l_T^2+(xP^+\nu)^2} + xP^+\nu} \right] \tag{15}$$

at $x \to 0$, with the factor $\nu = \sqrt{(v\cdot n)^2/n^2}$, which is finite because $n$ is not on the light cone. This is the reason $F$ does not acquire an explicit dependence on the large scale $P^+$ as

stated before, and the transverse degrees of freedom of a parton must be taken into account, leading to the $p_T$-factorization theorem [4]. The n dependence residing in Fig. l(c) then disappears with the vanishing of Eq. (15).

If neglecting the contribution from Fig. l(c), i.e., adopting $\bar{F} = \bar{F}_s$, Eq. (10) becomes

$$\frac{dF(x,p_T)}{d\ln(1/x)} = \bar{\alpha}_s(p_T)\int \frac{d^2l_T}{\pi l_T^2}\left[F(x,|p_T+l_T|) - \theta(p_T^2-l_T^2)F(x,p_T)\right], \tag{16}$$

which is exactly the BFKL equation adopted in [8]. Note that the BFKL equation has been written in various forms. The above form, though different from that appearing in [2], is simpler. The argument of $\bar{\alpha}_s$ has been set to the natural scale $p_T$. It is then understood that the subdiagram containing the special vertex plays the role of the evolution kernel. Obviously, the BFKL kernel is gauge invariant. After deriving the evolution equation, we make the vector $n^\mu$ approach $\delta^{\mu-}$, and the definition of $F$ returns to the standard one [14].

A careful examination reveals that it is not proper to extend the loop momentum $l^+$ of a real gluon to infinity when deriving Eq. (14), since the behavior of $F(x+l^+/P^+)$, vanishing at the large momentum fraction, should introduce an upper bound of $l^+$. To obtain a more reasonable evolution kernel, we propose to truncate $l^+$ at some scale, and a plausible choice of this scale is of order Q. The cutoff of $l^+$ introduces a n dependence. However, this n dependence can be absorbed into the cutoff, which will be regarded as a fitting parameter and be determined by the data of $F_2$ (for some value of Q). Then the gauge dependence does not appear explicitly in the modified evolution equation. It can be verified that the predictions are insensitive to the cutoff, and a good choice of the cutoff is $Q/(2\nu)$, where $\nu$ is the gauge factor appearing in Eq. (15). Performing the integration over $l^-$ and $l^+$, Eq. (14) becomes

$$\begin{aligned}\bar{F}_s(x,p_T,Q) = \frac{\bar{\alpha}_s}{2}\int \frac{d^2l_T}{\pi}\frac{-1}{l_T^2+4\nu^2 l^{+2}}\Big|_{l^+=0}^{l^+=Q/(2\nu)} \\ \times\left[F(x,|p_T+l_T|,Q) - \theta(p_T^2-l_T^2)F(x,p_T,\ Q)\right],\end{aligned} \tag{17}$$

where the Q dependence of $F$ from the constraint of phase space for the real gluon emission has been indicated. With this modification, the real gluon has smaller phase space at lower $Q$.

We derive the modified BFKL equation

$$\begin{aligned}\frac{dF(x,p_T,\ Q)}{d\ln(1/x)} =& \bar{\alpha}_s(p_T)\int \frac{d^2l_T}{\pi l_T^2}\left[F(x,|p_T+l_T|,\ Q) - \theta(p_T^2-l_T^2)F(x,p_T,\ Q)\right] \\ &- \bar{\alpha}_s(p_T)\int \frac{d^2l_T}{\pi}\frac{F(x,|p_T+l_T|,Q)}{l_T^2+Q^2},\end{aligned} \tag{18}$$

where the first and last terms correspond to the lower and upper bounds of $l^+$, respectively. Obviously, Eq. (18) approaches the conventional equation (16) in the $Q\to\infty$ limit. The first term on the right-hand side of Eq. (18) is responsible for the rise of $F$ at small x, and the last term acts to moderate the rise [11]. We then expect that the ascent of $F$ is slower at lower Q, for which the effect of the last term is stronger, and deviates from that predicted

by the conventional BFKL equation. Note that the $Q$ dependence in our formalism is attributed to the constraint of the phase space for radiative corrections, instead of to the $\ln Q$ summation.

### III. Evolution in x

Before proceeding with the numerical analysis, we extract the behavior of the gluon distribution function at small $x$ from the modified BFKL equation, and compare it with those from the DGLAP, BFKL, and CCFM equations. It will be observed that the modified BFKL equation and the CCFM equation give similar evolution in $x$. We reexpress Eq. (18) as [11]

$$\begin{aligned}\frac{dF(x,p_T,Q)}{d\ln(1/x)} = \bar{\alpha}_s \int \frac{d^2l_T}{\pi l_T^2}[F(x,|p_T+l_T|,Q) - \theta(Q_0^2-l_T^2)F(x,p_T,Q)] \\ -\bar{\alpha}_s \int \frac{d^2l_T}{\pi}\frac{F(x,|p_T+l_T|,Q)}{l_T^2+Q^2} .\end{aligned} \tag{19}$$

with a fixed coupling constant $\bar{\alpha}_s$. Note that the loop momentum $l_T$ in the virtual gluon emission is truncated at the scale $Q_0$, instead of at $p_T$. This modification is acceptable, since the virtual gluon contribution plays the role of a soft regulator for the real gluon emission, and setting the cutoff to $Q_0$ serves the same purpose. Furthermore, the replacement of $p_T$ by $Q_0$ allows us to solve Eq. (19) analytically using Fourier transform, such that the rough behavior of the small-$x$ evolution predicted by Eq. (18) can be extracted.

The Fourier transformation of Eq. (19) to the conjugate $b$ space leads to

$$\frac{d\tilde{F}(x,b,Q)}{d\ln(1/x)} = -S(b,Q)\tilde{F}(x,b,Q) , \tag{20}$$

with

$$S(b,Q) = 2\bar{\alpha}_s[\ln(Q_0b)+\gamma-\ln 2+K_0(Qb)] . \tag{21}$$

where the Bessel function $K_0$ comes from the last term on the right-hand side of Eq. (19), and $\gamma$ is the Euler constant. Equation (20) is trivially solved to give

$$\tilde{F}(x,b,Q) \propto \exp[-S(b,Q)\ln(x_0/x)] , \tag{22}$$

$x_0$ being the initial momentum fraction below which the gluon distribution function begins to evolve according to the BFKL equation Transforming Eq. (22) back to momentum space, we have

$$F(x,p_T,Q) = \int_0^\infty bdbJ_0(p_Tb)\tilde{F}(x,b,Q) . \tag{23}$$

Assuming that the above integral is dominated by the contribution from the small $b$ region, $F$ is expected to grow as

$$\tilde{F}(x,0,Q) \propto \exp[2\bar{\alpha}_s \ln(x_0/x)\ln(Q/Q_0)] \,. \tag{24}$$

This power-law rise with $1/x$ is steeper compared to the DGLAP evolution,

$$\exp\left[4\sqrt{\frac{N_c}{\beta_0}\ln\frac{1}{x}\ln\frac{\ln(Q/\Lambda_{QCD})}{\ln(Q_0/\Lambda_{QCD})}}\right] \,, \tag{25}$$

$\beta_0$ being the first coefficient of the QCD beta function, and is more sensitive to the variation of $Q$ compared to the conventional BFKL evolution,

$$\exp[4\ln 2\bar{\alpha}_s \ln(x_0/x)] \,. \tag{26}$$

Remind that the DGLAP evolution with $x$ is not strong enough, while the conventional BFKL rise is $Q$-independent. Equations (24)-(26) then hint that the modified BFKL equation can explain the data well.

At the same time, we shall study the CCFM equation, whose $Q$ dependence comes from the $\ln Q$ summation. It is written as

$$\begin{aligned} F(x,p_T,Q) = F^{(0)}(x,p_T,Q) + \int_x^1 dz \int \frac{d^2q}{\pi q^2}\theta(Q-zq)\Delta_S(Q,zq) \\ \times \tilde{P}(z,q,p_T)F(x/z,|p_T+(1-z)q|,q) \,, \end{aligned} \tag{27}$$

with the splitting function

$$\tilde{P} = \bar{\alpha}_s(p_T)\left[\frac{1}{(1-z)_+} + \Delta_{NS}(z,q,p_T)\frac{1}{z} + z(1-z)\right] \,. \tag{28}$$

The so-called "Sudakov" exponential $\Delta_S$ and the "non-Sudakov" exponentials $\Delta$ are given by

$$\begin{aligned} \Delta_S(Q,zq) &= \exp\left[-\bar{\alpha}_s \int_{(zq)^2}^{Q^2} \frac{dp^2}{p^2}\int_0^{1-p_T/p}\frac{dz'}{1-z'}\right] \,, \\ \Delta_{NS}(z,q,p_T) &= \exp\left[-\bar{\alpha}_s \int_z^{z_0}\frac{dz'}{z'}\int_{(z'q)^2}^{p_T^2}\frac{dp^2}{p^2}\right] \,. \end{aligned} \tag{29}$$

The upper bound $z_0$ of the variable $z'$ in Eq. (29) takes the values [7, 8],

$$z_0 = \begin{array}{ll} 1 & \text{if } 1 \le (p_T/q) \\ p_T/q & \text{if } z < (p_T/q) < 1 \\ z & \text{if } (p_T/q) \le z \,. \end{array} \tag{30}$$

The Sudakov exponential $\Delta_S$ collects the contributions from the rung gluons obeying the strong angular ordering, and is the result of the $\ln Q$ summation. Those gluons which do not obey the angular ordering are grouped into $\Delta_{NS}$. For the simpler derivation of the CCFM equation using the resummation technique, refer to [11]. In the small $x$ region we adopt the approximate form of the CCFM equation [8],

$$F(x,p_T,Q) = F^{(0)}(x,p_T,Q) + \bar{\alpha}_s(p_T)\int_x^1 \frac{dz}{z}\int \frac{d^2q}{\pi q^2}\theta(Q-zq)\theta(q-\mu) \times \Delta_{NS}(z,q,p_T)F(x/z,|p_T+(1-z)q|,q)\,. \tag{31}$$

The extra theta function $\theta(q-\mu)$ introduces an infrared cutoff of the variable $q$. The flat nonperturbative driving term $F^{(0)}$ will be defined later.

We extract the approximate CCFM evolution in $x$ as a comparision. Applying $d/d\ln(1/x)$ to both sides of Eq. (31) gives

$$\frac{dF(x,p_T,Q)}{d\ln(1/x)} \approx \bar{\alpha}_s\int_x^1 \frac{dz}{z}\int \frac{d^2q}{\pi q^2}\theta(Q-zq)\theta(q-\mu)\Delta_{NS}(z,q,p_T) \times \frac{d}{d\ln(1/x)}F(x/z,|p_T+q|,Q)\,. \tag{32}$$

Again, we assume a fixed coupling constant $\bar{\alpha}_s$. The derivative of the flat driving term $F^{(0)}$ has been dropped. The differentiation of the lower bound of $z$ vanishes, because of $F(\xi=1)=0$. The arguments $|p_T+(1-z)q|$ and $q$ of $F$ in the integrand have been replaced by $|p_T+q|$ and $Q$, respectively, for simplicity. The identity $dF/d\ln(1/x) = dF/d\ln z$ and the neglect of the derivatives of other factors in the integrand lead to

$$\begin{aligned}\frac{dF(x,p_T,Q)}{d\ln(1/x)} &\approx \bar{\alpha}_s\int_x^1 dz\frac{d}{dz}\int \frac{d^2q}{\pi q^2}\theta(Q-zq)\theta(q-\mu) \times \Delta_{NS}(z,q,p_T)F(x/z,|p_T+q|,Q)\,, \\ &= \bar{\alpha}_s\int \frac{d^2q}{\pi q^2}\theta(Q-q)\theta(q-\mu)F(x,|p_T+q|,Q)\,.\end{aligned} \tag{33}$$

To derive the last line of the above formulas, we have employed $F(\xi=1)=0$ and $\Delta_{NS}(1,q,p_T)=1$ according to Eq. (29). The Fourier transformation of the above equation is given by

$$\frac{d\tilde{F}}{d\ln(1/x)} \approx 2\bar{\alpha}_s\ln(Q/\mu)\tilde{F} \tag{34}$$

in the small $b$ region. It is obvious that the CCFM equation predicts a similar evolution in $x$ to Eq. (24). This similarity will be verified numerically in the next section. However, its $Q$ dependence is due to the transverse momentum ordering as indicated by the function $\theta(Q-q)$, a source different from the constraint on the longitudinal momenta of real gluons in the modified BFKL equation.

Another observation is that the CCFM equation gives a steeper rise at small $x$ than the DGLAP equation does. The reason is attributed to the different choices of the argument of the running coupling constant in the splitting function, which is $p_T$ in the former (see Eq. (28)) and $q$ in the latter. Hence, $\alpha_s(p_T)$ does not run in fact, as the variable $q$ is integrated over in the CCFM equation (31). While $\alpha_s(q)$ evolves to $\alpha_s(Q)$ when solving the DGLAP equation. Because of $\alpha_s(p_T) > \alpha_s(Q)$, the CCFM evolution is stronger.

## IV. Numerical results

We solve both the modified and conventional BFKL equations numerically following the repetation method proposed in [8] by starting with a "flat" gluon distribution function [8, 15],

$$F^{(i)}(x,p_T) = \frac{3}{Q_0^2} N_g (1-x)^5 \exp(-p_T^2/Q_0^2), \tag{35}$$

with $Q_0 = 1$ GeV. The active flavor number $n_f$ in the running coupling constant $\alpha_s$ is set to 4. The normalization constant $N_g$ will be determined by the data of the structure function $F_2(x,Q^2)$ at some $Q$, and then employed to make predictions for other $Q$. We solve Eqs. (16) and (18) with $F^{(i)}$ in Eq. (35) inserted into their right-hand sides. Substitute the obtained solution of $F$ into the right-hand sides of Eqs. (16) and (18), and solve them again. Repeat this procedure until a limit solution of $F$ is reached. In the numerical analysis we introduce a lower bound $p_T > 1$ GeV to avoid the infrared divergence in $\bar{\alpha}_s(p_T)$ from the $p_T$ diffusion at small $x$. The CCFM equation is also solved in a similar way with the driving term $F^{(0)}$,

$$\begin{aligned} F^{(0)}(x,p_T,Q) = {} & \frac{3}{Q_0^2} N_g \exp(-p_T^2/Q_0^2) \int_x^1 \frac{dz}{z} \theta(Q - z p_T) \\ & \times \Delta_{NS}(z,p_T,p_T) \frac{d(1-x/z)^5}{d\ln(z/x)}, \end{aligned} \tag{36}$$

wich reduces to $F^{(i)}$, when the functions $\theta$ and $\Delta_{NS}$ are set to unity.

The expressions of the structure functions $F_{2,L}$, according to the $p_T$-factorization theorem [4], are given by

$$F_2(x,Q^2) = \int_{xx}^1 \frac{d\xi}{\xi} \int_0^{p_c} \frac{d^2p_T}{\pi} H_2(x/\xi,p_T,Q) F(\xi,p_T,Q) + \frac{3}{2} F_L(x,Q^2), \tag{37}$$

$$F_L(x,Q^2) = \int_x^1 \frac{d\xi}{\xi} \int_0^{p_c'} \frac{d^2p_T}{\pi} H_L(x/\xi,p_T,Q) F(\xi,p_T,Q), \tag{38}$$

$p_c$ and $p_c'$ being the upper bounds of $p_T$ which will be specified later. The hard scattering subamplitudes $H_{2,L}$ denote the contributions from the quark box diagrams in Fig. 2, where both the incoming photon and gluon are off shell by $q^2 = -Q^2$ and $p^2 = -p_T^2$, respectively, $P = (\xi P^+, 0, p_T)$ being the parton momentum and $\xi$ the momentum fraction. They are written as

$$H_2 = e_q^2 \frac{\alpha_s}{\pi} C z \left\{ \left[ z^2 + (1-z)^2 - 2z(1-2z)\frac{p_T^2}{Q^2} + 2z^2 \frac{p_T^4}{Q^4} \right] \times \frac{1}{A} \ln \frac{1+A}{1-A} - 2 \right\}, \tag{39}$$

and $H_L = H_L^{a+b} + H_L^c$, with

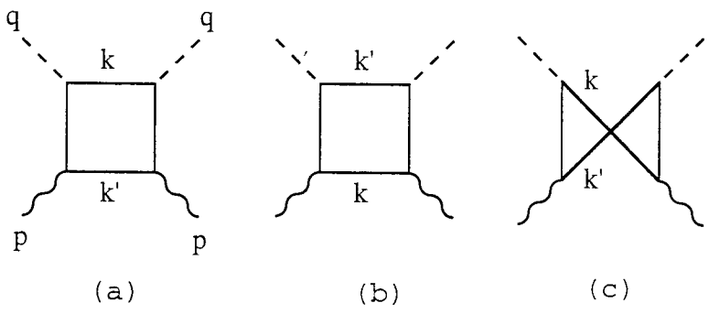


FIG. 2. The quark box diagrams contributing to the hard scattering subamplitudes $H_{2,L}$.

$$H_L^{a+b} = -2e_q^2\frac{\alpha_s}{\pi}Cz\left\{\frac{1}{2}-\frac{x}{z}+z\frac{p_T^2}{Q^2}\frac{B^2}{A^2}+\frac{2z^2}{A^2}\left[\left(1-2z\frac{p_T^2}{Q^2}\right)^2-2z\frac{p_T^2}{Q^2}B^2\right]\right.$$
$$\left.\times\left(\frac{p_T^2}{Q^2}-\frac{p_T^2}{Q^2}\frac{1}{A}\ln\frac{1+A}{1-A}+\frac{1}{4z^2}\right)\right\} \tag{40}$$

the sum of the contributions from Figs. 2(a) and 2(b), and

$$\begin{aligned}H_L^c = -2e_q^2\frac{\alpha_s}{\pi}Cz\Bigg\{&\left[\frac{x^2}{z}-2x^2\frac{p_T^2}{Q^2}\right.\\&\left.-\left(1-\frac{p_T^2}{Q^2}\right)\left(2zx-z-2z^2\frac{p_T^2}{Q^2}\frac{B^2}{A^2}\right)\right]\frac{1}{A}\ln\frac{1+A}{1-A}\\&-\left[(z-zx)\left(1-\frac{p_T^2}{Q^2}\right)\left(1-2z\frac{p_T^2}{Q^2}\right)-xA^2\right]\tfrac{1}{A^2}\ln\frac{1+A^2}{1-A^2}\\&-\left[2x\left(1-2z\frac{p_T^2}{Q^2}\right)-z\left(1-\frac{p_T^2}{Q^2}\right)\frac{1-2z(3-z)p_T^2/Q^2+6z^2p_T^4/Q^4}{A^2}\right]\\&\times\frac{1}{A^2}\left(\frac{1}{A}\ln\frac{1+A}{1-A}-2\right)\Bigg\}\end{aligned} \tag{41}$$

from Fig. 2(c). The factors $A$, $B$ and $C$ are $A=\sqrt{1-4z^2p_T^2/Q^2}$, $B=\sqrt{1-z-zp_T^2/Q^2}$ and $C=1/2$. The detailed derivation of $H_{2,L}$ is presented in the Appendix. We have assumed a vanishing charm quark mass for simplicity. To require $H_{2,L}$ be meaningful, the upper bounds of $p_T$ are set to

$$p_c=\min\left(Q,\frac{\xi}{2x}Q\right)\ ,\quad p_c'=\min\left(Q,\frac{\xi-x}{x}Q\right)\ . \tag{42}$$

The existence of the upper bounds of $p_T$ is natural from the viewpoint of PQCD factorization theorems: The partons entering the hard scattering amplitude should be roughly on-shell.

If $p_T$ is large, the gluon coming out of the proton will be highly off-shell, and can not be regarded as a parton. It is easy to observe that the terms in the braces of $H_2$ approaches the splitting function

$$P_{qg}(z) = C[z^2 + (1- z)^2] \tag{43}$$

in the $p_T \to 0$ limit.

We evaluate Eq. (37) for $Q^2 = 15\,\mathrm{GeV}^2$ with $F(\xi, p_T, \mathrm{Q})$ obtained from the modified BFKL equation, and then determine the normalization constant as $N_g = 3.29$ from the data fitting. When $Q^2$ varies, we adjust $N_g$ such that $xg$ has a fixed normalization $\int_0^1 \mathrm{xgdx}$. $F_2$ for $Q^2 = 8.5$, 12, 25, and 50 $\mathrm{GeV}^2$ are then computed, and results along with the HERA data [1] are displayed in Fig. 3. It is obvious that our predictions agree with the data well. The curves have a slower rise at smaller Q, which is the consequence of the phase space constraint for real gluon emissions. For comparision, we show the results from the conventional BFKL equation, and from the CCFM equation. The former are almost $Q$-independent, and close to those from the modified BFKL equation only at large $Q^2 = 50$ $\mathrm{GeV}^2$. Therefore, their match with the data is not very satisfactory, especially in the low Q region. The latter, also consistent with the data, are similar to those from the modified BFKL equation as expected.

The normalization constants $N_g$ for $F_2$ are then employed to evaluate the structure function $F_L(x, Q^2)$ using Eq. (38) for the corresponding Q. The predictions for $Q^2 = 8.5$, 12, 15, 25, and 50 $\mathrm{GeV}^2$ are presented in Fig. 4, which behave in a similar way to $F_2(x, Q^2)$, but are smaller in magnitude. Note that the uncertainty of the experimental data [16] shown in Fig. 4 is still large: The vertical lines adjacent to x $= 10^{-4}$ for $Q^2 = 8.5$ and 12 $\mathrm{GeV}^2$ represent the error bars. The central values slightly above 0.5 are outside of the plot range. Hence, it is not difficult to explain the current data. To draw a concrete conclusion, more precise data are necessary.

The gluon density xg is defined by the integral of the unintegrated gluon distribution function over $p_T$ [8],

$$xg(x, Q^2) = \int_0^Q \frac{d^2 p_T}{\pi} F(x, p_T, Q) \,. \tag{44}$$

The dependnece of $xg$ on x for $\mathrm{Q}^2 = 8.5$, 15, and 50 $\mathrm{GeV}^2$ derived from the modified BFKL equation is displayed in Fig. 5. If letting the parameter $\lambda$ characterize the behavior of xg $\sim x^{-\lambda}$ at small $x$, we find the values $\lambda \approx 0.3$ for $Q^2 = 8.5$ $\mathrm{GeV}^2$ and $\lambda \approx 0.4$ for $Q^2 = 50$ $\mathrm{GeV}^2$. The former is consistent with that obtained from a phenomenological fit to the HERA data [17]. The latter is close to that from solving the conventional BFKL equation numerically [18], i.e., from hard pomeron contributions. As explained before, the smaller $\lambda$ at lower Q is due to the more restricted phase space for real gluon emissions. The flat gluon density corresponding to soft pomeron exchanges can then be understood following this vein.

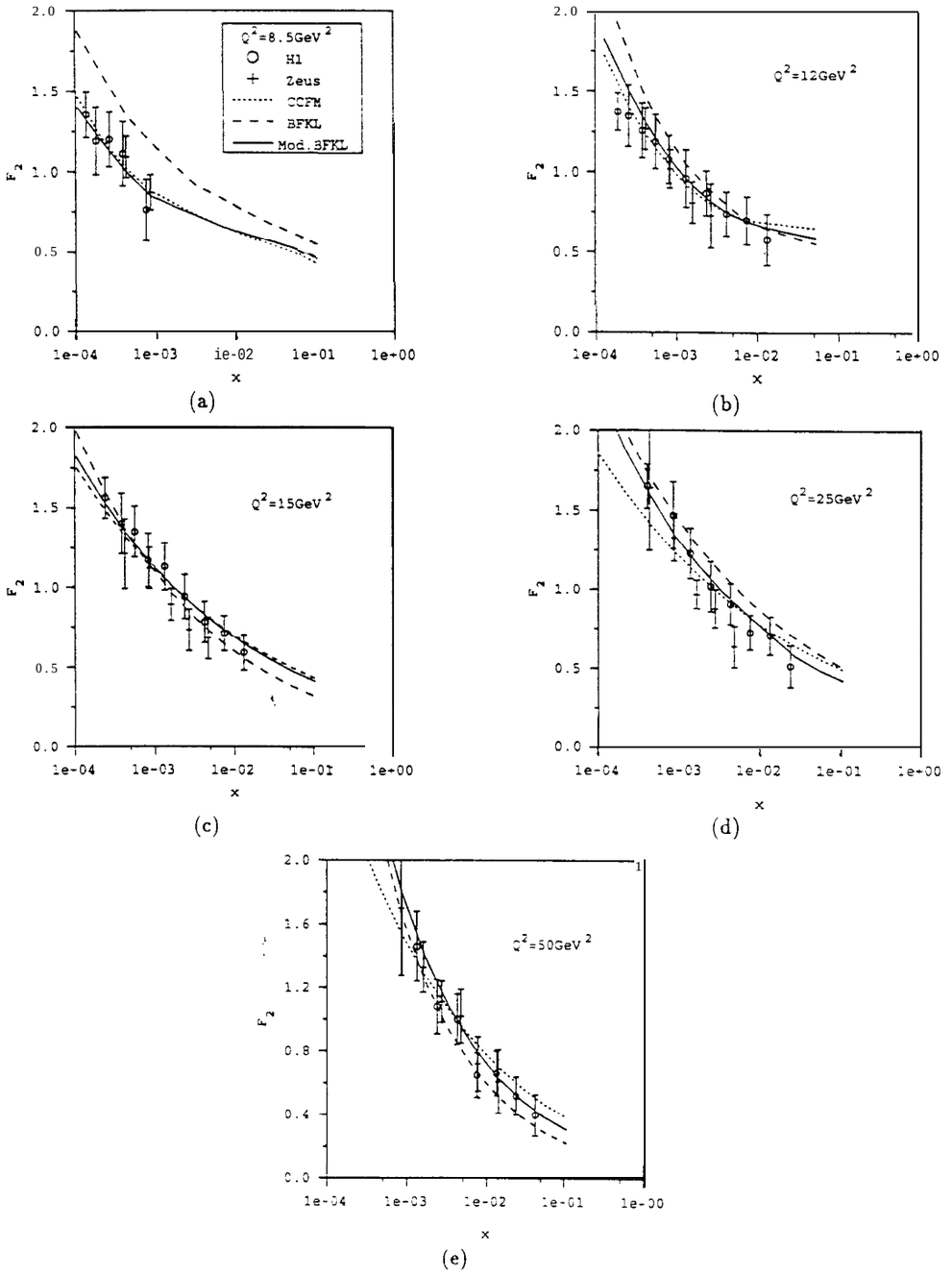


FIG. 3. The dependence of $F_2$ on x for $Q^2 = 8.5$, 12, 15, 25, and 50 GeV$^2$ derived from the modified BFKL equation, the conventional BFKL equation, and the CCFM equation. The HERA data [1] are also shown.

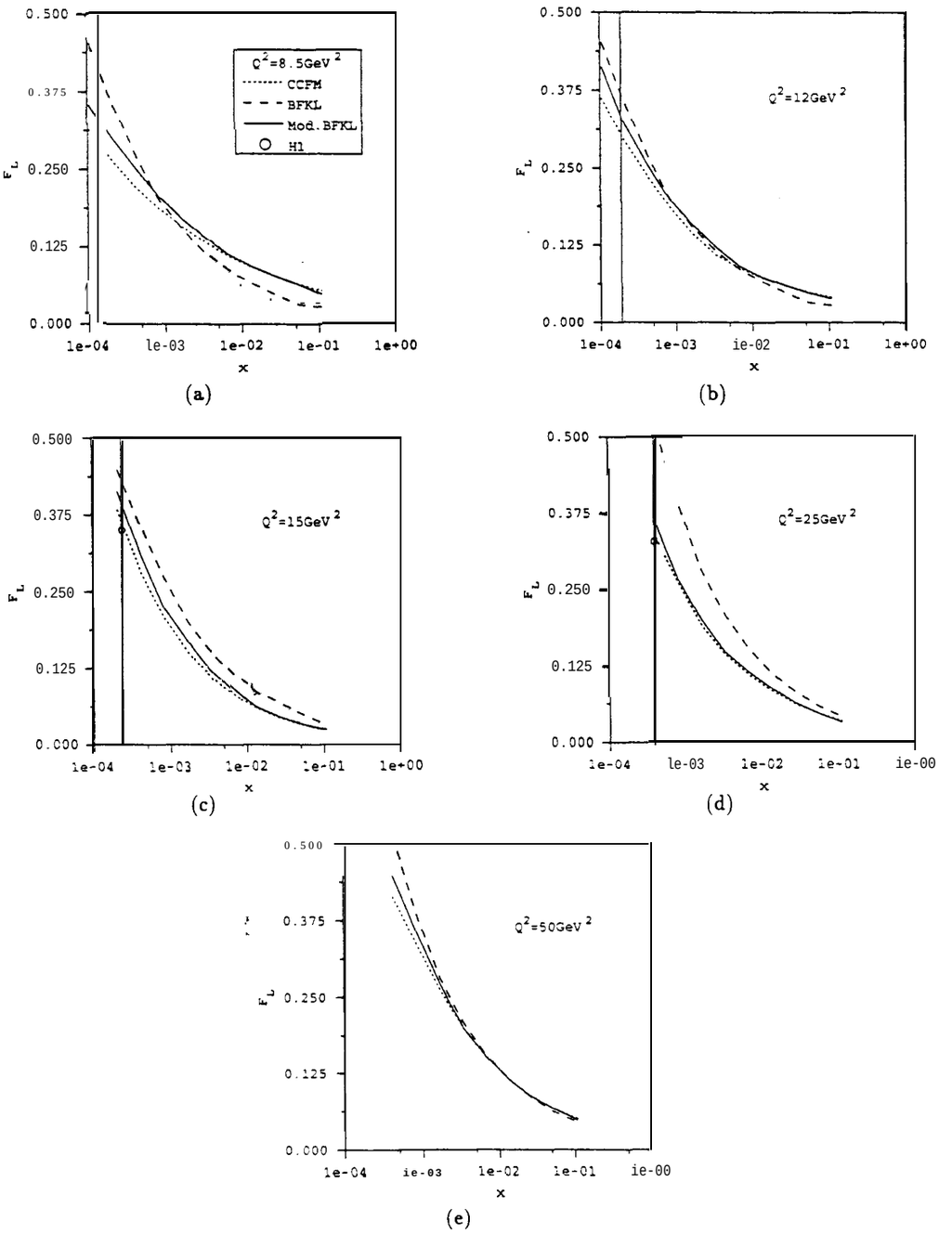


FIG. 4. The dependence of $F_L$ on $x$ for $Q^2 = 8.5$, 12, 15, 25, and 50 $GeV^2$ derived from the modified BFKL equation, the conventional BFKL equation, and the CCFM equation. The HERA data [16] are also shown.

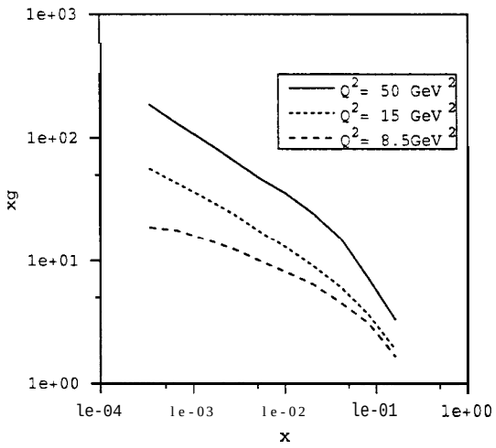


FIG. 5. The dependence of xg on x derived from the modified BFKL equation.

## V. Conclusion

In this paper we have studied in details the modified **BFKL** equation proposed from the viewpoint of the resummation technique. This equation possesses a $Q$ dependence from the constraint of the phase space for soft real gluon emissions. It gives rise to the desired behaviors in $x$ and in $Q$ of the gluon distribution function and the structure functions $F_{2,L}$, which are consistent with the **HERA** data. The predictions are close to those from the CCFM equation, whose Q dependence is, however, due to the $\ln Q$ summation. The rise of the gluon density at small $x$ predicted by the modified BFKL equation is steeper than that by the DGLAP equation, and is more sensitive to the variation of Q compared to that by the conventional BFKL equation. We have also explained why the conventional BFKL equation overestimates the real gluon contributions and thus the rise of the structure functions in the low Q region. Real gluons, responsible for the BFKL rise, in fact should have more restricted phase space at smaller Q.

This work demonstrates the simplicity and success of the resummation technique in the study of the DIS structure functions at small $x$. However, the power-law rise of the structure functions predicted by either the conventional or modified BFKL equation violates the unitarity bound [19]. A further application of our formalism to the issue of the unitarity of the BFKL evolution is referred to [20].

## Acknowledgments

This work was supported by the National Science Council of Republic of China under the Grant No. NSC87-2112-M-006-018.

## Appendix

In this Appendix we extract the hard scattering subamplitudes from the box diagrams in Fig. 2. The photon and gluon with the off-shell momenta $q^2 = -Q^2$ and $p^2 = -p_T^2$, respectively, annihilate into a quark with momentum $k$ and an antiquark with $k'$. These diagrams can be regarded as a parton-level cross section, which are then convoluted with the unintegrated gluon distribution function $F$ as shown in Eq. (37). The structure functions $F_{2,L}$ are extracted from the DIS hadronic tensor $W_{\mu\nu}$ through the contractions

$$\begin{aligned} -g^{\mu\nu}W_{\mu\nu} &= \frac{F_2}{x} - \frac{3}{2x}F_L \,, \\ P^\mu P^\nu W_{\mu\nu} &= \frac{Q^2}{4x^2}\frac{F_L}{2x} \,, \end{aligned} \tag{45}$$

where the longitudinal structure function $F_L$ is, in terms of the standard ones $F_{1,2}$, written as $F_L = F_2 - 2xF_1$.

In the infinite-momentum frame of the proton, the only nonvanishing component of $P$ is $P^+$, and the gluon carries the parton momentum $\xi P^+ + p_T$. In the center-of-mass frame of the photon and gluon, the gluon momentum is transformed into $p$ with the space component $p$ in the $z$ direction. The relation $q + p = 0$ leads to

$$q_0^2 = q^2 + |q|^2 = -Q^2 + |p|^2 = p_0^2 - p^2 - Q^2 \,. \tag{46}$$

From the parton-level Bjorken variable

$$z = \frac{x}{\xi} = \frac{Q^2}{2p\cdot q} = \frac{Q^2}{2(p_0 q_0 + |p|\,|q|)} \,, \tag{47}$$

with Eq. (46) inserted, we solve for $p_0$, which is expressed as

$$p_0 = \frac{Q}{2}\frac{1 + 2zp^2/Q^2}{\sqrt{z(1 - z + zp^2/Q^2)}} \,. \tag{48}$$

It is then easy to obtain

$$|p| = \frac{Q}{2}\frac{\sqrt{1 + 4z^2p^2/Q^2}}{\sqrt{z(1 - z + zp^2/Q^2)}} \,, \tag{49}$$

$$q_0 = \frac{Q}{2}\frac{1 - 2z}{\sqrt{z(1 - z + zp^2/Q^2)}} \,. \tag{50}$$

Since each of the quarks shares half of the total energy, we have

$$k_0 = k_0' = \frac{1}{2}(p_0 + q_0) = \frac{Q}{2}\frac{1 - z + zp^2/Q^2}{\sqrt{z(1 - z + zp^2/Q^2)}} \,. \tag{51}$$

Similarly, the invariants $s = (p + q)^2$, $t = (p - k')^2$ and $u = (p - k)^2$ are written as

$$
\begin{aligned}
s &= \frac{Q^2}{x}\left(1-z+z\frac{p^2}{Q^2}\right) , \\
t &= -\frac{Q^2}{2z}\left(1+\sqrt{1+4z^2\frac{p^2}{Q^2}}\cos\theta\right) , \\
u &= -\frac{Q^2}{2z}\left(1-\sqrt{1+4z^2\frac{p^2}{Q^2}}\cos\theta\right) ,
\end{aligned}
\tag{52}
$$

where $\theta$ is the angle between the momenta $k$ and $p$.

We first compute $-g^{\mu\nu}\hat{W}_{\mu\nu}$, where $\hat{W}_{\mu\nu}$ is the parton-level hadronic tensor. Contracting $-g^{\mu\nu}$ to the box diagrams, the squared amplitude from Fig. 2(a) is given by

$$
(-g^{\mu\nu}\hat{W}_{\mu\nu})_a = \frac{1}{4}e_q^2 g^2 C Tr\left[\not{k}'\gamma_\nu\frac{\not{k}-\not{q}}{(k-q)^2}\gamma_\mu\ \not{k}\gamma^\mu\frac{\not{k}-\not{q}}{(k-q)^2}\gamma^\nu\right] , \tag{53}
$$

where the factor $1/4$ denotes the average over the spins of the photon and gluon, $C = 1/2$ is the color factor from the identity $Tr(T^aT^b) = (1/2)\delta^{ab}$, $T^{a,b}$ being the color matrices, and $e_q$ is the charge of the quark $q$ in unit of $e$. A straightforward calculation leads to

$$
(-g^{\mu\nu}\hat{W}_{\mu\nu})_a = 8\pi e_q^2\alpha_s C\left(\frac{tu+p^2Q^2}{t^2}\right) . \tag{54}
$$

Since Fig. 2(b) is idential to Fig. 2(a) under the interchange of $k$ and $k'$, we have $(-g^{\mu\nu}\hat{W}_{\mu\nu})_b = (-g^{\mu\nu}\hat{W}_{\mu\nu})_a(t \leftrightarrow u)$. A similar evaluation of Fig. 2(c) gives

$$
(-g^{\mu\nu}\hat{W}_{\mu\nu})_c = 8\pi e_q^2\alpha_s C\left[\frac{s(p^2-Q^2)}{tu}\right] . \tag{55}
$$

The complete expression is then written as

$$
\begin{aligned}
-g^{\mu\nu}\hat{W}_{\mu\nu} &= (-g^{\mu\nu}\hat{W}_{\mu\nu})_a + (-g^{\mu\nu}\hat{W}_{\mu\nu})_b + (-g^{\mu\nu}\hat{W}_{\mu\nu})_c , \\
&= 8\pi e_q^2\alpha_s C\left[\frac{u}{t}+\frac{t}{u}+\frac{p^2Q^2}{t^2}+\frac{p^2Q^2}{u^2}+\frac{2s(p^2-Q^2)}{tu}\right] .
\end{aligned}
\tag{56}
$$

Next we calculate the contraction $P^\mu P^\nu W_{\mu\nu}$. Note that the proton momentum $P$ is not parallel to the gluon momentum $p$, because the gluon is off shell, while the proton is on shell. In the center-of-mass frame $P$ possesses different components from those in the infinite-momentum frame. From the invariants,

$$
\begin{aligned}
&P\cdot p = P_0p_0 - P_3|p| = 0 , \\
&x = z\xi = \frac{Q^2}{2P\cdot q} = \frac{Q^2}{2(P_0q_0+P_3|q|)} ,
\end{aligned}
\tag{57}
$$

the components $P_0$ and $P_3$ in the center-of-mass frame are solved to be

$$
\begin{aligned}
P_0 &= \frac{Q}{2\xi}\frac{1}{\sqrt{z(1-z+zp^2/Q^2)}}, \\
P_3 &= \frac{Q}{2\xi}\frac{1+2zp^2/Q^2}{\sqrt{z(1-z+zp^2/Q^2)}\sqrt{1+4z^2p^2/Q^2}}.
\end{aligned}
\tag{58}
$$

Because of $P^2 = 0$, it is easy to obtain the transverse components

$$
P_T = \frac{p_T^2}{\xi^2}\frac{1}{1+4z^2p^2/Q^2}. \tag{59}
$$

It will be found that all the contributions from Fig. 2 to $P^\mu P^\nu W_{\mu\nu}$ can be expressed in terms of the invariant,

$$
P\cdot k = P_0k_0 - P_3k_0\cos\theta - P_Tk_0\sin\theta\cos\phi, \tag{60}
$$

with

$$
\begin{aligned}
P_0k_0 &= \frac{Q^2}{4x}, \\
P_3k_0 &= \frac{Q^2}{4x}\frac{1+2zp^2/Q^2}{\sqrt{1+4z^2p^2/Q^2}}, \\
P_Tk_0 &= \frac{p_TQ}{2x}\frac{\sqrt{z(1-z+zp^2/Q^2)}}{\sqrt{1+4z^2p^2/Q^2}},
\end{aligned}
\tag{61}
$$

$\phi$ being the azimuthal angle of the momentum $k$. Following a similar procedure, we derive the squared amplitudes from Figs. 2(a), 2(b) and 2(c),

$$
\begin{aligned}
\left(P^\mu P^\nu \hat{W}_{\mu\nu}\right)_a &= 8\pi e_q^2\alpha_s C\frac{p^2}{t^2}\left[2(P\cdot k)^2 - \frac{Q^2}{z}P\cdot k\right], \\
\left(P^\mu P^\nu \hat{W}_{\mu\nu}\right)_b &= \left(P^\mu P^\nu \hat{W}_{\mu\nu}\right)_a (t\leftrightarrow u), \\
(P^\mu P^\nu W_{\mu\nu})_c &= -8\pi e_q^2\alpha_s C\frac{1}{tu}\left\{2(Q^2+p^2)(P\cdot k)^2\right. \\
&\quad -\frac{Q^2}{z}\left[Q^2+p^2-\frac{Q^2}{2z}A\cos\theta\right]P\cdot k \\
&\quad \left.+\frac{Q^4}{4z^2}\left[\frac{Q^2}{2z}(1-A\cos\theta)+p^2\right]\right\},
\end{aligned}
\tag{62}
$$

respectively, with $A = \sqrt{1+4z^2p^2/Q^2}$. The complete expression is given by

$$
P^\mu P^\nu \hat{W}_{\mu\nu} = \left(P^\mu P^\nu \hat{W}_{\mu\nu}\right)_a + \left(P^\mu P^\nu \hat{W}_{\mu\nu}\right)_b + \left(P^\mu P^\nu \hat{W}_{\mu\nu}\right)_c. \tag{63}
$$

To extract the hard scattering subamplitudes, we integrate Eqs. (56) and (62) over phase space. For $-g^{\mu\nu}\hat{W}_{\mu\nu}$ which is independnet of the azimuthal angle $\phi$, the integral is written as

$$\begin{aligned} H_2 &= \frac{1}{2\pi}\frac{1}{(2\pi)^4}\int d^4k'd^4k\delta^4(p+q-k-k') \\ &\quad \times 2\pi\delta_+(k^2)2\pi\delta_+(k'^2)z(-g^{\mu\nu}\hat{W}_{\mu\nu}), \\ &= \frac{1}{32\pi^2}\int d\cos\theta z(-g^{\mu\nu}\hat{W}_{\mu\nu}). \end{aligned} \tag{64}$$

Substituting Eq. (56) into Eq. (64) and integrating it over cos $\theta$, we obtain Eq. (39), where the relation $p^2 = -p_T^2$ has been inserted. For another contraction $P^\mu P^\nu W_{\mu\nu}$, which depends on $\phi$, the integral is given by

$$H_L = \frac{1}{64\pi^3}\int d\cos\theta d\phi 2z\frac{4x^2}{Q^2}P^\mu P^\nu \hat{W}_{\mu\nu}. \tag{65}$$

After a tedious calculation, we obtain Eqs. (40) and (41).

## References


[1] ZEUS Collaboration, M. Derrick et al., Z. Phys. **C65**, 379 (1995); H1 Collaboration, T. Ahmed *et al.*, Nucl. Phys. B439, 471 (1995).

[2] E. A. Kuraev, L. N. Lipatov and V. S. Fadin, Sov. Phys. JETP 45, 199 (1977); Ya. Ya. Balitskii and L. N. Lipatov, Sov. J. Nucl. Phys. 28, 822 (1978); L. N. Lipatov, Sov. Phys. JETP 63, 904 (1986).

[3] V. N. Gribov and L. N. Lipatov, Sov. J. Nucl. Phys. 15, 428 (1972); G. Altarelli and G. Parisi, Nucl. Phys. B126, 298 (1977); Yu.L. Dokshitzer, Sov. Phys. JETP 46, 641 (1977).

[4] T. Jaroszewicz, Acta. Phys. Pol. **B11**, 965 (1980); S. Catani, M. Ciafaloni, and F. Hautmann, Phys. Lett. B242, 97 (1990); Nucl. Phys. **B366**, 657 (1991); S. Catani and F. Hautmann, Nucl. Phys. B427, 475 (1994).

[5] R. K. Ellis, F. Hautmann, and B. R. Webber, Phys. Lett. B348, 582 (1995).

[6] R. D. Bail and S. Forte, Phys. Lett. B335, 77 (1994); 336, 77 (1994).

[7] M. Ciafaloni, Nucl. Phys. B296, 49 (1988); S. Catani, F. Fiorani, and G. Marchesini, Phys. Lett. B234, 339 (1990); Nucl. Phys. B336, 18 (1990); G. Marchesini, Nucl. Phys. B445, 49 (1995).

[8] J. Kwiecinski, A. D. Martin, and P.J. Sutton, Phys. Rev. D52, 1445 (1995); 53, 6094 (1996).

[9] J. C. Collins and D. E. Soper, Nucl. Phys. **B193**, 381 (1981).

[10] H-n. Li, Phys. Lett. B405, 347 (1997).

[11] H-n. Li, Phys. Lett. B416, 192 (1998); Chin. J. Phys. 37, 8 (1999).

[12] L. V. Gribov, E. M. Levin and M. G. Ryskin, Nucl. Phys. **B188**, 555 (1981); Phys. Rep. 100, 1 (1983).

[13] H-n. Li, Phys. Rev. D55, 105 (1997).

[14] H-n. Li, Report No. hep-ph/9803202.

[15] P. D. B. Collins and F. Gault, Phys. Lett. **B112**, 255 (1982); A. Donnachie and P. V. Landshoff, Nucl. Phys. B244, 322 (1984); Nucl. Phys. B267, 690 (1986).

[16] H1 Collaboration, Report No. ISSN 0418-9833; A. De Roeck, presented at the International Symposium on QCD Corrections and New Physics, Hiroshima, Japan, 1997.

[17] A. D. Martin, R. G. Roberts, and W. J. Stirling, Phys. Rev. D50, 6734 (1994); Phys. Lett. B354, 155 (1995).

[18] A. J. Askew, *et* al., Phys. Rev. D49, 4402 (1994); J. R. Forshaw, R. G. Roberts, and R. S. Thorne, Phys. Lett. B356, 79 (1995).

[19] P. D. B. Collins and E. J. Squires, Regge *Poles in Particle Physics,* Springer Tracts in Modern Physics, ' Vol. 45 (Springer-Verlag, Berlin, 1968).

[20] H-n. Li, Report No. hep-ph/9709236, Phys. Lett. B429, 121 (1998).